Narrow photoemission lines from graphite valence states

T. Kihlgren,[1] T. Balasubramanian,[2] L. Walldén,[1] and R. Yakimova[3]
[1]*Physics Department, Chalmers University of Technology, Göteborg, Sweden*
[2]*MAX-lab, Lund University, Lund, Sweden*
[3]*Department of Physics and Measurement Technology, Linköping University, Linköping, Sweden*
(Received 4 June 2002; revised manuscript received 27 September 2002; published 31 December 2002)

Valence-band photoelectron angular distributions, measured in the photon energy range 20−150 eV, are obtained from crystalline graphite overlayers prepared by heating SiC(0001) and from a graphite natural single crystal. The dispersion of the valence bands for the overlayers agrees well with that of the single crystal. The valence electrons have binding energies, which agree with LDA calculations if the calculated binding energies are multiplied by a factor of 1.13. The upper σ state at Γ and states near the Fermi level at the zone corners give quite narrow emission lines. Since the widths are on par with that of the C 1*s* level the lines are of interest as an alternative to the core line when graphite is used as substrate for adsorption or absorption studies.

DOI: 10.1103/PhysRevB.66.235422 PACS number(s): 73.21.−b

I. INTRODUCTION

Stimulated by the recent observation using low-energy electron diffraction (LEED) that crystalline surface layers of graphite can be prepared by heating SiC crystals[1] we have recorded angle-resolved photoemission spectra to probe the valence states of such layers and also for a natural single crystal. The overlayers are of interest as an alternative to natural single crystals, which are inconveniently small for many experiments. After noting that the overall valence band dispersion in high symmetry directions of the overlayers agrees well with previous results for natural single crystals[2,3] we have used the samples to search for narrow emission lines. Such lines are valuable for observing adsorbate or absorbate induced binding energy shifts when these shifts are small. Of obvious interest in this respect are the states near the Fermi energy, which are found near the corners of the Brillouin zone. The band structure is complicated in this region but is of main interest since the states are involved in the electron transfer to or from an adsorbate or absorbate and important for electron transport properties. In a search for narrow emission lines another state of interest is the upper σ state at the center of the Brillouin zone. This state marks a band maximum, which means that only Auger processes of interband type can contribute to the decay of the photohole. For a semimetal one furthermore expects this decay to be slow due to the low density of states in the vicinity of the Fermi level.

Electron lifetimes in graphite are of general interest due to the marked deviation from Fermi liquid theory observed in experiments covering the range 0–2.4 eV above the Fermi level.[4,5] The anomalous behavior was ascribed to the anisotropic band structure of graphite.[5,6] Since this should influence also hole lifetimes the linewidths measured in the present work ought to be of interest for further modelling. Furthermore graphite has high vibration frequencies which is favourable for observing the influence on the line shape of the electron-phonon interaction when states near the Fermi level are probed.[7,8]

II. EXPERIMENTAL

The experiments were performed at beamline 33 in the MAX synchrotron radiation facility, Lund, Sweden. The beamline is equipped with a spherical grating monochromator and an end station with a 75 mm radius electron analyzer with variable angular resolution down to $\pm 0.4°$. The experimental energy resolution for the spectra taken is, if not stated otherwise, around 60 meV. An incidence angle of 45° was chosen for the experiment. One set of samples was prepared by *in situ* heating of *n*-doped 6H-SiC(0001) as described by Fourbaux *et al.*[1] Before insertion in the experimental chamber these samples were rinsed in HF solution. The samples were then heated in ultrahigh vacuum by a dc current. The temperature, measured with a pyrometer, was increased to 1450 °C in steps such that the various surface reconstructions[1,9] could be monitored by LEED. The heating was continued well beyond the time where the Si 2*p* photoemission line observed at $h\nu = 150$ eV was no longer detected. Most spectra presented below for graphite overlayers were measured from samples prepared *in situ.* The spectral profile produced by the states near the *K* point is intricate and somewhat better resolved using an overlayer sample prepared in a separate oven. This sample is an off axes (8°) cut 4H-SiC(0001) crystal, which was heated to a significantly higher temperature, around 2000 °C, in a graphite enclosure and at 1 atm. argon pressure. The sample was then kept in air before insertion into the photoemission chamber and heated to 980 °C prior to measurements. The LEED pattern and STM images (Fig. 1) from this sample show that there are two different facets with an angle of around 160° between them.

The two facets give two sets of photoemission spectra. Nevertheless the spectral features of each facet can easily be identified due to the large angle between the facets. The intensity of the LEED pattern shows that one facet is stronger and according to the STM images this orientation consists of larger and rather flat terraces. Of further interest is that each of the facets gives a threefold LEED pattern, indicative of perfect termination, whereas a sixfold pattern is observed for the samples prepared *in situ* and also for the natural crystal.

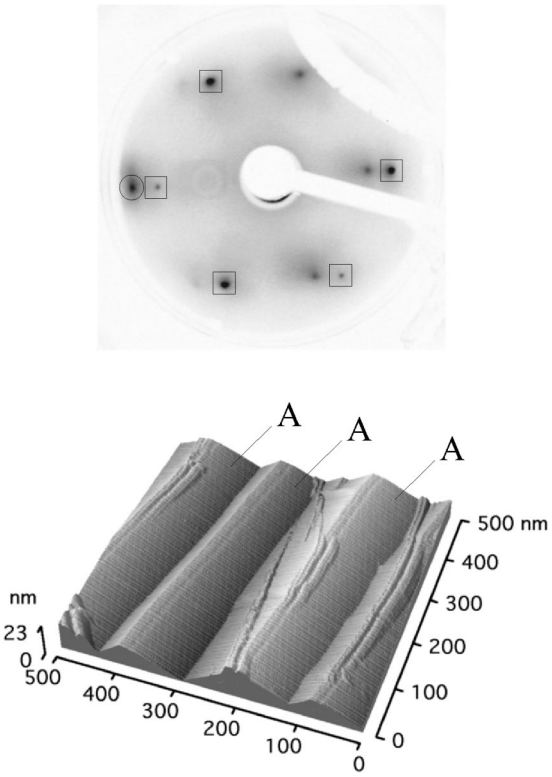

FIG. 1. (a) LEED pattern obtained with the electrons ($E = 122$ eV) incident normally to the terraces marked by A in the lower panel. The LEED spots marked by squares are obtained from this facet and the spot marked by a circle is the (00) spot from the second facet. (b) STM image of the off-axis cut (8°) 4H-SiC(0001) sample showing terraces of graphite (500 nm×500 nm).

Compared to the terraced sample those prepared in situ are rough, according to the STM measurements, consisting of a large number of terraces with different heights.

III. RESULTS AND DISCUSSION

A. Overall band structure

Figure 2 shows binding energies measured in the Γ-*K* and Γ-*M* symmetry directions plotted versus the parallel wave vector component of the emitted electrons. The photon energies are 46 and 70 eV. Included also in Fig. 2 is a band structure based on a calculation using the local density approximation with the full-potential linear muffin-tin-orbital (FPLMTO) method[10] with the binding energies multiplied by 1.13 such that the calculated band bottom (19.2 eV below E_F) coincides with our experimental value (21.7 eV). The bandwidth is in excellent agreement with experimental results and quasiparticle calculations performed by Heske *et al.*,[11] who found a widening of the valence band in graphite compared to the local-density approximation (LDA) calculations. As for the maximum of upper σ band, Ref. 10, gives a value of 3.4 eV, which when multiplied by 1.13 gives 3.84 eV, rather close to our experimental value of 4.1 eV. It should however be mentioned that the degree of agreement obtained with the simple stretching picture (Fig. 2), depends on which one of the many band structure calculations reported for graphite the comparison is made with. As an example of the scatter in the calculated band energies, a table in Ref. 10 of previously calculated energies shows values in the range from 3.0 to 4.6 eV for the maximum of the upper σ band. More recent calculations give energies near 3.0 eV (Refs. 12,13) which according to the simple stretching picture gives a value of 3.39 eV clearly suggesting that the future refinements on the simple stretching picture is needed.

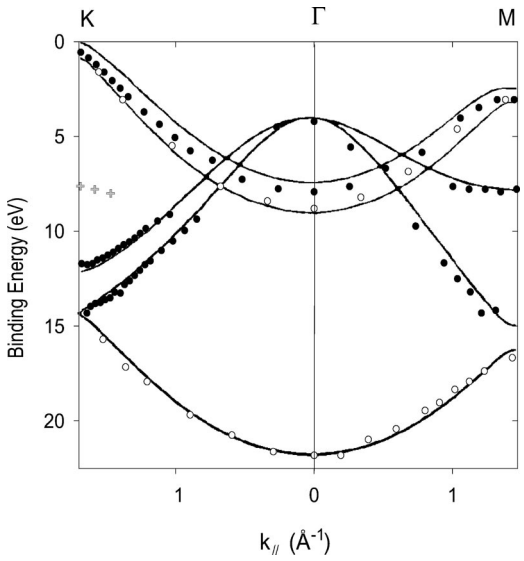

FIG. 2. Plot of binding energy vs $k_{//}$ in symmetry directions for an in situ prepared sample. The filled and open circles are the experimentally determined points corresponding to 46 and 70 eV photon energy respectively. The line is a band structure calculated by local density approximation (Ref. 10), where the calculated binding energy has been stretched by 13 % (see text for details). The crosses, obtained with $h\nu = 46$ eV, is due to an anomalous peak shown in Fig. 4.

For σ states the dispersion along the *c* axis ($k_\perp$) is insignificant so the plot in Fig. 2 gives the in-plane dispersion of the σ states. Since the π states disperse with $k_\perp$, the π state binding energies plotted in Fig. 2 are merely representative of the two photon energies used. The binding energy of the π state measured in the normal direction at different photon energies is shown in Fig. 3(a) and the full width at half maximum of the emission line is shown in Fig. 3(b). The dispersion of the π states along the *c* axis and in lateral high symmetry directions agrees well with earlier work on single crystals[2,3] as well as with our own results for a natural crystal. Comparison with the stretched LDA calculation in Fig. 2 shows agreement for the minimum binding energy of the dispersing π band. Our experimental value of 8.9 eV should be compared to 8.8 eV, which is the value of the binding energy given in Ref. 10 multiplied by the factor 1.13. The agreement is less for the maximum binding energy of the dispersing band.

In a recent photoemission study of graphite thermally grown on SiC the interest was focused on the width of the π state observed in normal emission at photon energies between 23 and 55 eV.[12] From the data a lifetime broadening of 3.8 eV was obtained, varying insignificantly with the photon energy. However, as shown in Fig. 3(b), the peak width var-

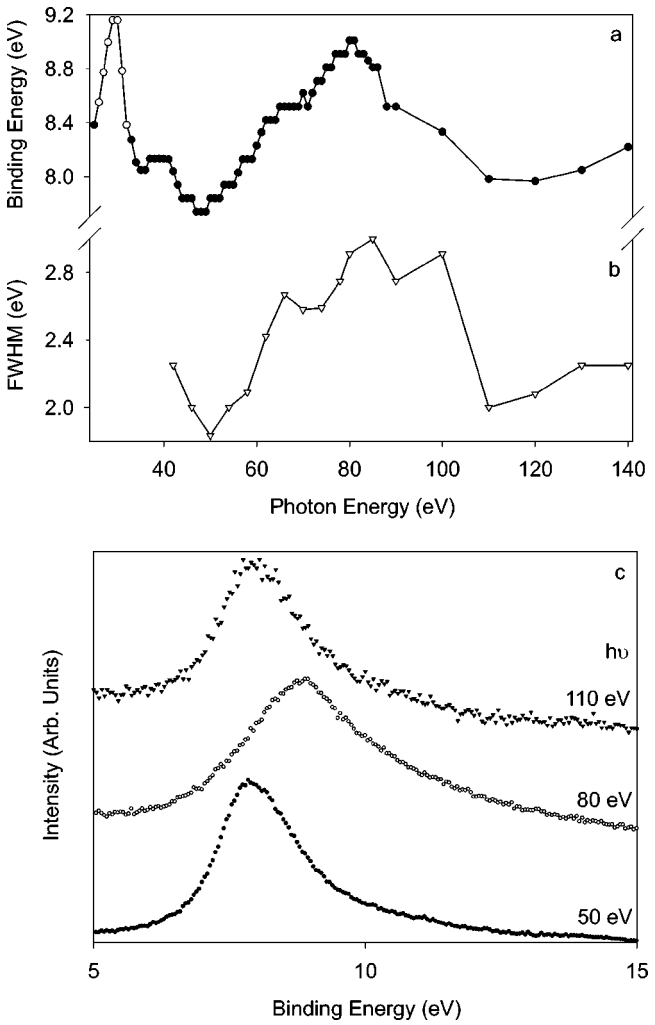

FIG. 3. Two panels, both for *in situ* prepared samples. (a) Binding energy measured along the surface normal versus photon energy for the π band (larger uncertainty in energy for unfilled circles). (b) the width (FWHM) of the π-emission line. (c) π-emission line at 50, 80, and 110 eV photon energy.

ies within the band from around 1.9 eV at minimum binding energy to 2.9 eV at maximum binding energy. A sample of spectra for the π state in normal emission is shown in Fig. 3(c). One can notice that at the higher photon energies used here the emission peak is less distorted by final state effects, which are probably responsible for the larger width noted by Strocov *et al.*[12] The bottom σ state (no spectrum shown) gives a line width of 2.7 eV.

Figure 4 shows a strong and dispersive peak at around 7.5 eV binding energy near the corners of the Brillouin zone (see also Fig. 2). We observe this peak at different photon energies $h\nu=46$ and 70 eV, for *in situ* and *ex situ* prepared samples as well as for the natural single crystal although it is more distinct for the terraced sample. This peak, which was observed also in previous work,[3] is anomalous since it has no counterpart in the calculated band structure. In the measured photoemission spectra we have not noticed any influence of the additional period introduced by the ordered step terraces.

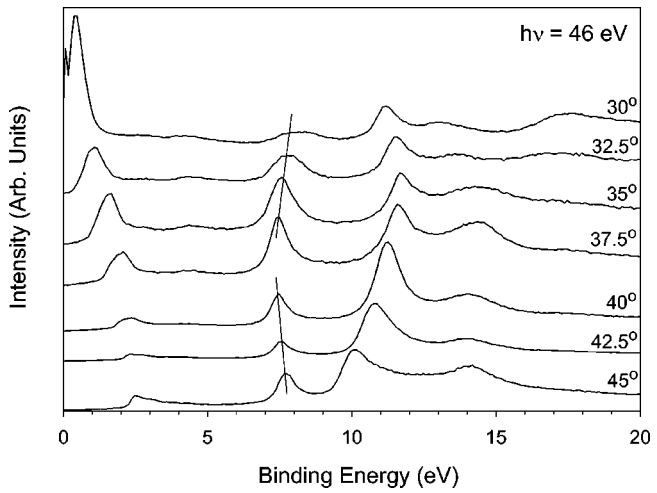

FIG. 4. Photoemission spectra at different polar angles of the *ex situ* prepared sample showing an anomalous peak (marked) indicating the existence of states near zone corners with a binding energy of around 7.5 eV. The spectra are recorded along Γ-*K*-*M*, parallel to the incident plane. At a polar angle of 35° the anomalous peak has a parallel wave vector near the zone corner.

B. The upper σ state

Figure 5(a) shows the upper σ state, at 4.1 eV binding energy, measured at the Γ points in the first and second Brillouin zones with the incidence plane parallel to Γ-*K* and the detector perpendicular to the incidence plane. Compared to the π line at 7.9 eV binding energy, a quite small intensity is recorded for the upper σ state at Γ in the first zone, but when the detector is instead positioned to observe the state in the second Brillouin zone it dominates the emission [Fig. 5(a)]. The state gives an asymmetric line with a narrow low binding energy side (83 meV at half maximum) and a wide tail towards high binding energies. This width is observed when the sample is at 100 K and the line is slightly narrower than at room temperature.

The width for the upper σ state is on par with that measured for the C 1*s* core level (160 meV) in graphite[14] but the σ line is more asymmetric. The core level emission was found to have two components. This was ascribed to a bulk-surface split 1*s* binding energy with 120 meV higher binding energy for C atoms in the surface layer.[14] The C 1*s* spectra, which were recorded along the surface normal at different photon energies extending to 65 eV above the 1*s* excitation threshold, show that the surface component gives the stronger signal, by a factor of 5 or more. The σ states in adjacent layers have an insignificant overlap one could expect a bulk-surface split binding energy also for the upper σ state but this we do not observe.

In the first zone, emission from the upper σ-state appears only above a threshold photon energy of around 36 eV [Fig. 5(c)]. The narrow σ line then appears on the low binding energy side of a broader peak, which is observed already at $h\nu=20$ eV and gains strength as the photon energy exceeds approximately 30 eV. In previous work the narrow σ line was not resolved and the broader peak was assigned to the σ state.

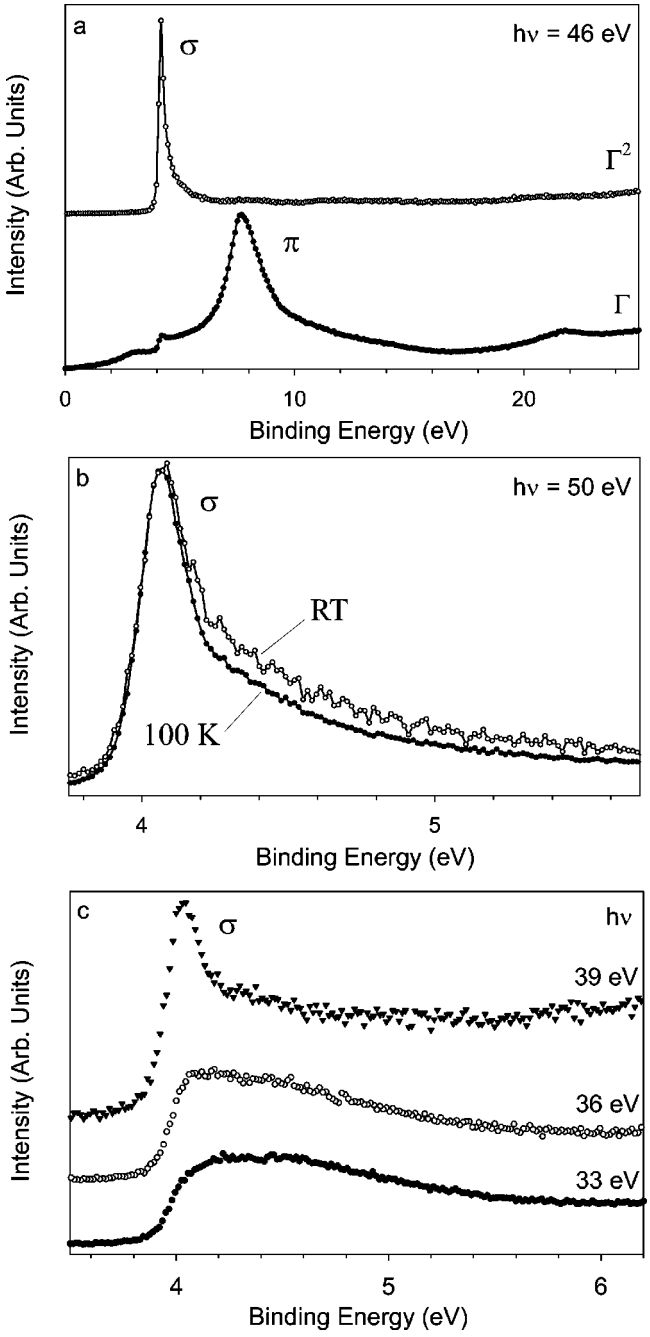

FIG. 5. Photoelectron energy spectra, all for *in situ* samples except for the upper spectrum in (a) which is measured for the terraced sample. (a) Normal emission (lower spectrum) and spectrum recorded with the detector set at 67.5° polar angle to probe the upper σ state in the second zone in a plane normal to the plane of incidence (upper spectrum). (b) The σ line in the second Brillouin zone at RT and at 100 K. (c) The upper σ line recorded along the surface normal at three different photon energies.

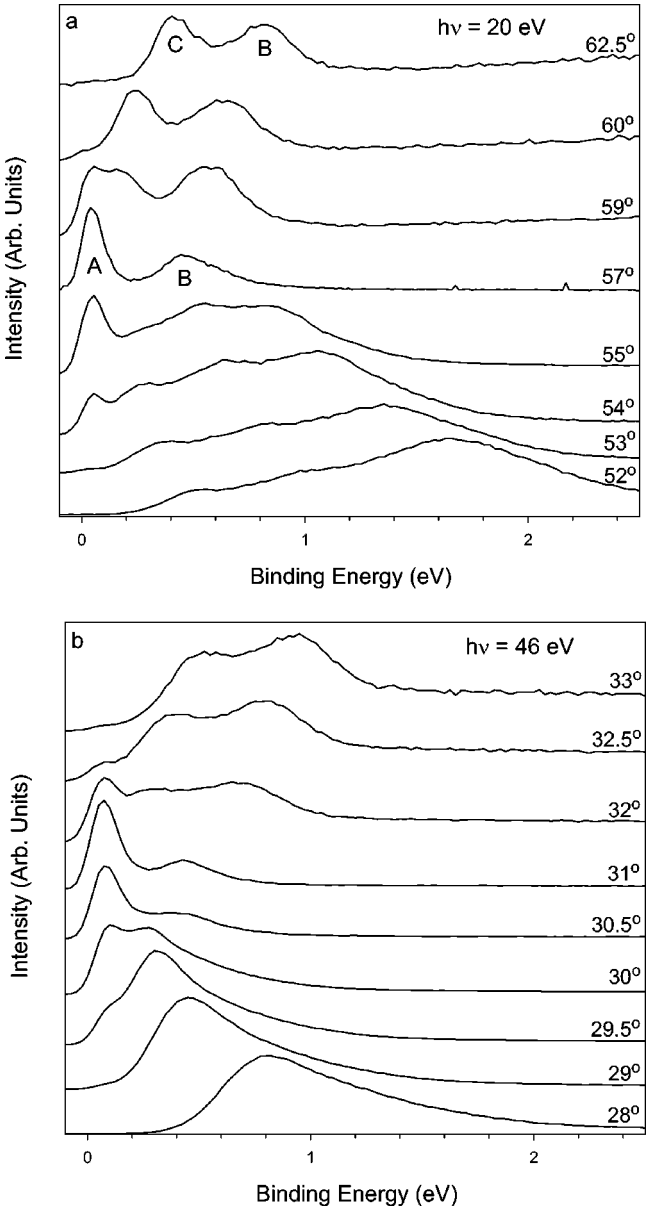

FIG. 6. Angle resolved spectra of the *ex situ* prepared sample at different polar angles choosen to probe states along Γ-*K*-*M* near the *K* point. (a) $h\nu = 20$ eV (57° corresponds to K). (b) $h\nu = 46$ eV (31° corresponds to K).

In a plane wave approximation for the final state no emission is expected from the σ state in spectra recorded along the surface normal.[15] The reason is that the state changes sign across the surface such that there are equally large positive and negative contributions to the photoemission matrix element. Our observation of a threshold photon energy of 36 eV suggests that the appearance of the σ line can be explained by including diffracted waves in the final state. At $h\nu = 36$ eV the final energy is 32 eV above the Fermi level. In a recent very-low-energy electron diffraction experiment an energy band characterized by strong hybridization with off-normal diffracted waves was found to give an onset of absorption at 33 eV for normally incident electrons.[13] The emergence of the narrow σ line may therefore be explained by transitions into this band. The interpretation of the broad peak on the high binding energy side of the σ line is uncertain. The binding energy suggests that the emission is due to σ band states in the vicinity of Γ. The observation of strong emission from the σ state in the second zone (Fig. 5) is in accordance with observations of Shirley *et al.*[15] and Daimon *et al.*[16]

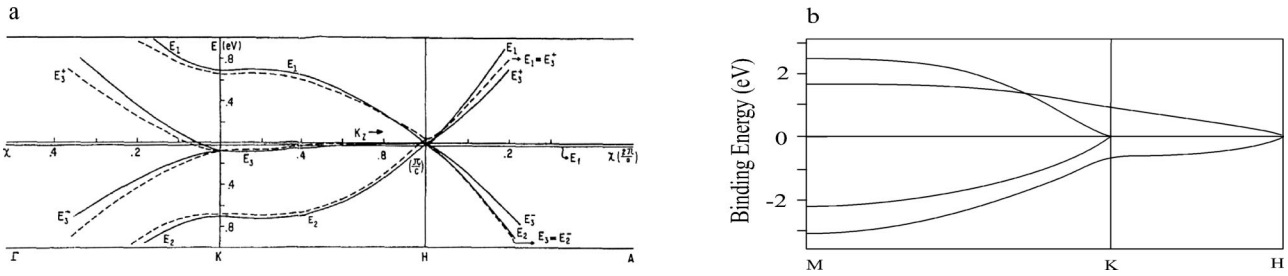

FIG. 7. (a) Details of band structure calculations along different symmetry directions around the Fermi level (a) (SWMc) (Ref. 20), (b) (FPLMTO) (Ref. 10).

The linewidth for the upper σ state at Γ is an order of magnitude smaller than the widths for the π states at Γ and the bottom σ state. An obvious reason for this is that the quenching of the photohole proceeds by Auger processes of different type. The hole in the π and bottom σ state can be filled via intraband Auger processes. These are typically more effective than interband processes, which are the only possible ones for the upper σ state since this makes a band maximum. As recently found for electrons with energies near above E_F (Refs. 5,6) the unusual electronic structure of graphite will affect also hole lifetimes. The minute density of states at E_F in graphite and the low density within a couple of eV of E_F means a further reduction of the rate at which a hole in the upper σ state is filled. The π and the lower σ states are at lower energies and line widths are therefore expected to be less influenced by the density of states in a range near E_F.

C. States near E_F

In addition to the narrow σ line, a sharp line is resolved for the π electrons close to the Fermi level. To our knowledge this has not been noted in previous work. A sample of spectra is shown in Fig. 6. With the azimuthal detection angle in the Γ-*K*-*M* direction one finds that a narrow emission peak [A in Fig. 6(a)] appears at near zero binding energy for polar angles set to observe states close to a corner of the Brillouin zone. As the polar angle exceeds 57° and states beyond *K* are probed at $h\nu=20$ eV, peak A rapidly looses intensity. Peak B shifts to higher binding energies together with a new peak C such that the energy separation between the two remains nearly constant as the polar angle is changed.

The two peaks B and C reflect the two bands predicted for the *K*-*M* direction outside the zone corner [Fig. 7(b)]. The development of the spectral features is similar, with one exception, when the angular dependence is measured at different photon energies in the range 20–46 eV [for example, $h\nu=46$ eV in Fig. 6(b)]. At 35 eV only one peak is observed beyond the corner of the Brillouin zone. A possible reason is that with a photon energy of 35 eV the emission is from states close to the *H* point, where there is only one band outside the zone corner.[17] The peaks C and B have a separation of about 0.4 eV at photon energies in the ranges 20–30 eV and 40–46 eV. The energy separation between peak A and B near the zone corner is also measured to be 0.4 eV for $h\nu=20$–46 eV. The electronic structure near the Fermi energy and the shape of the Fermi surface is often described by the SWMc parameters.[18,19] From the different parameter values reported, the following values of the separation between the two bands at the *K* point are 0.52,[17] 0.58,[20] 0.67,[21] 0.80 eV (Ref. 22) and the lower of the two bands along *K*-*M* is 0.54,[17] 0.59,[20] 0.69,[21] 0.81 eV (Ref. 22) below the Fermi level at the *K* point. The latter energies can be compared with the binding energy of 0.46 eV for peak B in Fig. 6(a).

At photon energies, above 46 eV, the acceptance angle ($\pm 0.8°$) of the detector makes *k*-parallel selection too crude to measure accurately the rapid spectral variation near the zone corner. Even at $h\nu=20$ eV the strong angular dependence makes it difficult to monitor the changes in binding energy and intensity with the desired resolution. As may be noted in Fig. 6, the spectral changes can be large even when the change in angle is less than the acceptance angle. While the spectra are similar for the different samples, the features due to states near the zone corner with small binding energy are clearer in the spectra obtained for the *ex situ* prepared sample. In particular peak A at near zero binding energy is better resolved. The linewidth is 90 meV (FWHM), which is obtained with an experimental resolution of 50 meV. No significant change of the width is observed upon cooling the sample to 100 K. We ascribe peak A to the E_3^+ band (see Fig. 7). The Fermi surface of graphite lies within 0.077 $Å^{-1}$ (Ref. 20) of the corner of the Brillouin zone. The range of emission angles for which peak A is observed corresponds to a $k_{//}$ range of 0.096 $Å^{-1}$, in fair agreement with the expected range of populated wave vectors near the Fermi energy. For a further comparison with the Fermi surface models one notes in Fig. 6(a) that peak A disappears abruptly as the polar detection angle is increased from 59° to 60° and states outside the zone corner are probed. A cut of the Fermi surface with $k_z=0$ shows a triangular shape[20,22] which is consistent with the rapid disappearance of peak A beyond the corner of the zone.

Although the spectra are quite similar at the zone corner for the different photon energies, the spectral features at lower polar angles are rather different, as shown in Fig. 6. At $h\nu=20$ eV [Fig. 6(a)], the π band emerges from slightly higher binding energies when the angle is increased compared to $h\nu=46$ eV [Fig. 6(b)]. This difference in binding energy may be explained by the dispersion of the π states along the *c* axis in the manner observed when the binding energies of π electrons are measured along the surface normal at different photon energies. A possible explanation for

the difference is then, at $h\nu = 20$ eV states near the lower band [E_2 in Fig. 7(a)] are detected while at $h\nu = 46$ eV the emission is from states near the upper band [E_3^- in Fig. 7(a)].

IV. SUMMARY

In summary we find that there are narrow emission lines in the valence band photoemission spectrum of graphite. The width of the line due to the upper σ state is similar to that measured for the C 1*s* core level. This makes the σ state of interest as an alternative to the 1*s* level for adsorption and absorption studies. The linewidth of the σ state should also be of interest for hole lifetime estimates in a near 2D case where intraband Auger-processes are prohibited and the phase space for interband processes limited due to the semimetal character of graphite. Another narrow line, at near zero binding energy, demonstrates that photoemission can be used to resolve details of the electronic structure near Fermi level in graphite. Of experimental interest is that graphite overlayers prepared by heating SiC at high temperature give photoemission spectra with a quality that compare quite well with those recorded for natural single crystals.

ACKNOWLEDGMENT

Financial support from the Swedish Research Council is greatly acknowledged.

[1] I. Forbeaux, J.-M. Themlin, and J.-M. Debever, Phys. Rev. B **58**, 16 396 (1998).
[2] D. Marchand, C. Frétigny, M. Lagues, F. Batallan, Ch. Simon, I. Rosenman, and R. Pinchaux, Phys. Rev. B **30**, 4788 (1984).
[3] A.R. Law, M.T. Johnson, and H.P. Hughes, Phys. Rev. B **34**, 4289 (1986).
[4] S. Xu, J. Cao, C.C. Miller, D.A. Mantell, R.J.D. Miller, and Y. Gao, Phys. Rev. Lett. **76**, 483 (1996).
[5] G. Moos, C. Gahl, R. Fasel, M. Wolf, and T. Hertel, Phys. Rev. Lett. **87**, 267402 (2001).
[6] C.D. Spataru, M.A. Cazalilla, A. Rubio, L.X. Benedict, P.M. Echenique, and S.G. Louie, Phys. Rev. Lett. **87**, 246405 (2001).
[7] M. Hengsberger, R. Fresard, D. Purdie, P. Segovia, and Y. Baer, Phys. Rev. B **60**, 10 796 (1999).
[8] S. LaShell, E. Jensen, and T. Balasubramanian, Phys. Rev. B **61**, 2371 (2000).
[9] P. Mårtensson, F. Owman, L.I. Johansson, Phys. Status Solidi B **202**, 501 (1997).
[10] R. Ahuja, S. Auluck, J. Trygg, J.M. Wills, O. Eriksson, and B. Johansson, Phys. Rev. B **51**, 4813 (1995).
[11] C. Heske, R. Treusch, F.J. Himpsel, S. Kakar, L.J. Terminello, H.J. Weyer, and E.L. Shirley, Phys. Rev. B **59**, 4680 (1999).
[12] V.N. Strocov, A. Charrier, J.-M. Themlin, M. Rohlfing, R. Claessen, N. Barrett, J. Avila, J. Sanchez, and M.-C. Asensio, Phys. Rev. B **64**, 075105 (2001).
[13] V.N. Strocov, P. Blaha, H.I. Starnberg, M. Rohlfing, R. Claessen, J.-M. Debever, and J.-M. Themlin, Phys. Rev. B **61**, 4994 (2000).
[14] T. Balasubramanian, J.N. Andersen, and L. Walldén, Phys. Rev. B **64**, 205420 (2001).
[15] E.L. Shirley, L.J. Terminello, A. Santoni, and F.J. Himpsel, Phys. Rev. B **51**, 13 614 (1995).
[16] H. Daimon, M. Kotsugi, K. Nakatsuji, T. Okuda, and K. Hattori, Surf. Sci. **438**, 214 (1999).
[17] R.C. Tatar and S. Rabii, Phys. Rev. B **25**, 4126 (1982).
[18] J.C. Slonczewski and P.R. Weiss, Phys. Rev. **109**, 272 (1958).
[19] J.W. McClure, Phys. Rev. **108**, 612 (1957); **119**, 606 (1960).
[20] N.J. Luiggi and W. Barreto, Phys. Rev. B **34**, 2863 (1986).
[21] M.S. Dresselhaus and G. Dresselhaus, Adv. Phys. **30**, 139 (1981).
[22] J.-C. Charlier, X. Gonze, and J.-P. Michenaud, Phys. Rev. B **43**, 4579 (1991).